Energy 179 (2019) 581–592

Contents lists available at ScienceDirect

Energy

journal homepage: www.elsevier.com/locate/energy

Potential for energy and emissions of asymmetric twin-scroll turbocharged diesel engines combining inverse Brayton cycle system

Dengting Zhu, Xinqian Zheng*

Turbomachinery Laboratory, State Key Laboratory of Automotive Safety and Energy, Tsinghua University, Beijing, 100084, China

ARTICLE INFO

Article history:
Received 4 December 2018
Received in revised form
14 March 2019
Accepted 4 May 2019
Available online 9 May 2019

Keywords:
Diesel engine
Asymmetric twin-scroll turbocharging
Inverse Brayton cycle
Combined cycle
EGR rate
Power improvement

ABSTRACT

In this paper, a new combined cycle of asymmetric twin-scroll turbocharged diesel engine cycle and inverse Brayton cycle (IBC) for use is proposed. The use of a single asymmetric twin-scroll turbocharged diesel engine cycle is simple in structure and can improve the trade-off between low fuel consumption and nitrogen oxide emissions; however, both the engine exhaust gas recirculation (EGR) rate and the exhaust energy utilization should be further improved. A test bench experiment was performed to validate the numerical models of the single-cycle and combined-cycle approaches. Based on the models, the influence laws of the critical system parameters (turbine asymmetry and the IBC turbine throat area) on the engine performance characteristics were studied. The combined cycle was found to achieve improvements in both the engine EGR rate and the power. Given the same EGR rates at different engine speeds, the power improvement of the combined cycle was found to increase with increasing engine speed and decreasing turbine asymmetry, reaching a maximum of 5.00%. Moreover, further power improvements with an increasing IBC turbine throat area were observed, with the maximum power improvement of 5.78%. Compared with the power turbine, the combined cycle can utilize more waste heat at low and medium engine speeds; thus, the combined cycle is well-suited for use in heavy-duty diesel engines. The new combined cycle described in this report has great potential to provide substantial gains in both engine emissions and energy.

1. Introduction

Achieving high fuel economy and reduced exhaust emission levels are the major challenges of today's automobile industry [1]. During the last two decades, the large amount of fuel consumed by engines has led to the generation of a considerable amount of environmental pollution. Nowadays, energy conservation and emission reduction are very significant tasks to complete [2]. Compared with Euro 1 emissions legislation, Euro 6 has reduced nitrogen oxide (NO_x) by 95% [3]. To meet strict regulations on emissions and fuel consumption, some ways like exhaust gas recirculation (EGR), turbocharging technologies, and exhaust recovery systems are chosen [4,5].

The EGR technique is one of the most effective methods currently available for reducing NO_x emissions in internal combustion engines [6,7]. The EGR introduces part of the exhaust into the cylinder for combustion, reducing the oxygen content of the mixture [8,9]; with increasing EGR rates, the in-cylinder pressure peak decreases and the heat release for the combustion is delayed [10,11]. Roy et al. [12] concluded that turbocharging and EGR system control had a lot of improvements for emissions and fuel economy; the control approach decreased NO_x by over 50% relative to Euro 5. Currently, many turbocharging technologies, including variable geometry turbine (VGT), two-stage turbocharging, and asymmetric twin-scroll turbine (ATST) are widely combined with EGR in diesel engines.

VGTs and two-stage turbochargers are the two mature technologies currently used for recycling waste energy and driving EGR [13,14]. An engine equipped with a VGT has small movable blades to guide incoming exhaust through turbine blades. The blades angles change to optimize the exhaust flow [15,16]. Hatami et al. [17] carried out the optimization design of VGT blade geometry by applying the central composite design based on the experimental design, which exhibited an isentropic efficiency of 76.31%. An experimental study was conducted with a heavy-duty commercial diesel engine to investigate the coupling between dual loop EGR and VGT, and the results demonstrated that VGT and high pressure

* Corresponding author.
E-mail address: zhengxq@tsinghua.edu.cn (X. Zheng).

https://doi.org/10.1016/j.energy.2019.05.028
0360-5442/

EGR both significantly influenced turbocharger efficiency [18]. Moreover, the two-stage turbocharging is made up of two turbochargers that can be used for engine fuel consumption and NO_x reductions while achieving power upgrades [19,20]. The two-stage turbocharging approach offers flexibility to meet the requirements in the entire operating range of the engine versus the single-stage turbocharging [21,22]. However, both technologies described above have very complex control systems. For the same production volume, the cost of a typical VGT is from 270% to 300% the cost of the same-size, fixed-geometry turbocharger [23,24]. Two-stage turbocharging systems also have larger flow passage volume and more metal surfaces than single-stage systems [25].

The ATST is a new and promising turbocharging technology that can be used to meet the stringent targets for exhaust gas emissions. Originally, the twin-scroll turbine was proposed in 1954 [26] to improve the potential of the pulsating turbine operating mode. The practical benefit of a twin-scroll turbine is the reduction of the engine transient period and the enhancement of the exhaust gas pulse energy utilization rate [27]. This design goes beyond the traditional turbocharger design, which typically only accounts for steady-flow performance and enables improvement of the turbocharger design to achieve enhanced pulsed-flow turbine performance [28,29].

In the last century, the ATST was first implemented by Daimler-Benz to ensure the overall fuel consumption increase is as low as possible for the 6-cylinder truck engines equipped with an EGR system [30]. Daimler has launched the ATSTs for all its new diesel engines that are to meet the Euro 6 emission standard [31]. The heavy-duty diesel engines equipped with ATSTs include the 14.8L OM472, 12.8L OM471, 15.6L OM473 and 10.7L OM470 [32], which have NO_x emissions and fuel economy advantages [33]. Typically, the asymmetric twin-scroll turbocharged engine has one EGR circuit linked with the small volute to drive the EGR [34]. In Ref. [35], an experimental investigation of an asymmetric turbocharged diesel engine was performed. The results showed the following: compared to the symmetric twin-scroll turbine, the ATST had great potential for lower fuel consumption and emissions. Therefore, the ATST is a well-accepted choice for waste energy recovery and emissions decrease. Moreover, Zhu et al. [36] presented a new ATST with two wastegates (WGs), resulting in the maximum fuel economy improvement of 2.91% compared with the ATST with one WG.

To further improve fuel economy and reduce emissions, the inverted Brayton cycle (IBC) is one of the available technologies that can be used [37]. The IBC has been studied regarding its use in various applications for a number of years. In 1984, Wilson proposed and explained the operation of an IBC that consisted of totally inversed processes compared with the traditional Brayton cycle (BC) [38]. Agnew et al. [39] and Bianchi et al. [40] found that with higher inlet pressures in the IBC system, the energy efficiency could be enhanced. Zhang et al. [41] established a thermodynamic model IBC system and found that the power output reached a maximum as a function of the IBC compressor inlet pressure. As reported in Reference [42], regenerative BC and IBC were modified by partially bypassing the airflow entering the regenerator; the results showed that, from an operational point of view, more favorable output power with reasonable thermal efficiency could be generated by adjusting the bypass mass flow ratio. Chen et al. [43,44] validated a 1D model of a downsized spark ignition (SI) engine that was built as the baseline model to quantify the performance improvement; the experimental results showed that the system can generate a specific work of up to 17 kJ/kg, which proved out that the IBC system could achieve positive energy improvements compared with the engine with no IBC. The mechanical energy from the IBC turbine is useful. For example, it can be used to feed batteries which can supply energy to electric units like superchargers, start and stop systems or other electric units in the vehicle.

This work represents the first presentation of a combined cycle involving an asymmetric twin-scroll turbocharged diesel engine cycle and an IBC. Compared with the single cycle (only asymmetric twin-scroll turbocharged diesel engine cycle) and the power turbine, the combined cycle has higher EGR rate and improved exhaust energy utilization. This paper mainly describes the study of the influences of the critical parameters and exploits the potential of the combined cycle; the study consists of three parts. First, the combined cycle system is operated and analyzed, an engine experiment of an asymmetric twin-scroll turbocharged engine is presented, and the numerical models are validated. Second, both effect laws of the asymmetric turbine asymmetry and the IBC turbine throat area on the engine performance are investigated. Finally, the potential of the combined cycle is discussed compared with the power turbine.

2. System analysis

2.1. Asymmetric twin-scroll turbocharging system

Normally, the asymmetric twin-scroll turbocharging system provides more energy recovery and less NO_x to internal combustion engines [35]. This system is well-accepted for multi-cylinder diesel engines. The models of symmetric and asymmetric twin-scroll turbines are shown in Fig. 1. The conventional symmetric twin-scroll turbine is designed to make full use of the impulse energy and has two identical scrolls that generally exhibit an approximately symmetric exhaust gas flow behavior [45]. For the asymmetric twin-scroll turbine, the two scrolls have different throat areas. A parameter called turbine asymmetry (ASY) can be defined as the ratio of the large scroll throat area (TA_l) and the small scroll throat area (TA_s).

$$ASY = \frac{TA_s}{TA_l} \tag{1}$$

During the on-engine application, the different entries of a multiple-scroll turbine are meant to be connected to different engine cylinder groups of alternating firing order (shown in Fig. 2). Usually, a high exhaust gas back-pressure can be achieved for driving a high EGR rate in the turbine small scroll. Moreover, the turbine large scroll is not linked with the EGR circuit and can realize a lower average back-pressure, which is better for pumping loss

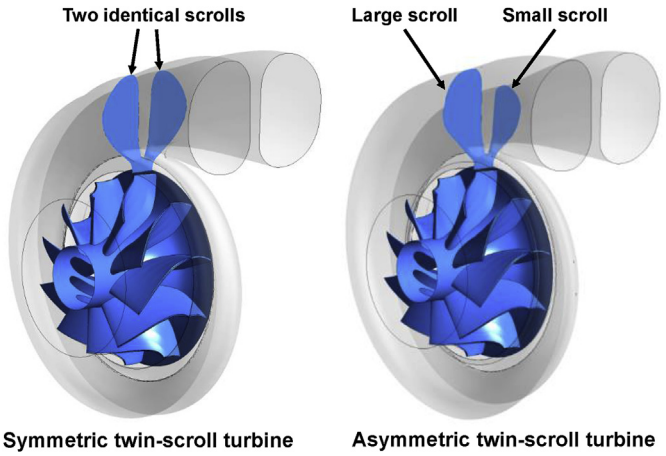

Fig. 1. Models of symmetric and asymmetric twin-scroll turbines.

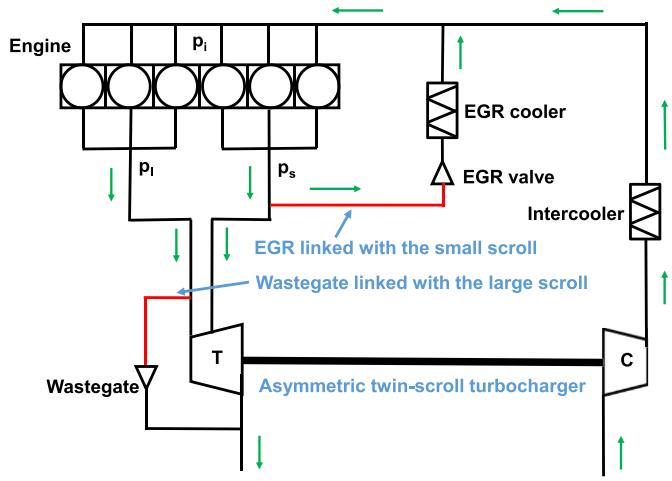

Fig. 2. A schematic of a 6-cylinder asymmetric twin-scroll turbocharged diesel engine.

and fuel consumption reduction. Generally, the pressures of the engine intake (p_i), the turbine small scroll (p_s) and the large scroll (p_l) satisfy the following relationships:

$$p_s > p_i \tag{2}$$

$$p_l < p_i \tag{3}$$

A WG device is attached to the turbine large scroll. At low engine load conditions, the WG is fully closed, and all exhaust gas will boost turbocharging. Because of the reduced volute area, the small scroll still has enough pressure to drive EGR. As the engine load increases, the exhaust energy will push the WG open gradually to prevent the over boost-pressure condition.

2.2. IBC system

The IBC system is a promising technology to further recovery of engine waste energy. For a single-stage IBC system (Fig. 3), three components (a compressor, a heat exchanger and a turbine) are used. The main processes are given as follows:

First, in the turbine, the waste gas is further expanded to sub-atmospheric pressure. On the one hand, the power of the turbine is partially utilized for compression work in the compressor, and on the other hand, the turbine has the mechanical energy left over which can be exported by a shaft. Therefore, giving the turbine isentropic efficiency (η_t), the specific work of the turbine is defined as:

$$P_t = m(h_1 - h_2)\eta_t \tag{4}$$

Next, the heat exchanger cools the exhaust gas from the turbine; such cooling is beneficial to reduce the energy consumption of the compressor. The cooling efficiency (ε) (defined as Eq. (5) according to Fig. 3) and the pressure loss of the heat exchanger are two significant parameters that mainly depend on the heat exchanger design.

$$\varepsilon = \frac{T_2 - T_3}{T_2 - T_0} \tag{5}$$

Finally, the exhaust gas is boosted to the environmental pressure by the compressor. The waste power of the compressor is given by

$$Pc = \frac{m(h_4 - h_3)}{\eta c} \tag{6}$$

Hence, the power of the IBC system can be described as (mechanical efficiency η_m):

$$P_{IBC} = P_t\eta_m - P_c \tag{7}$$

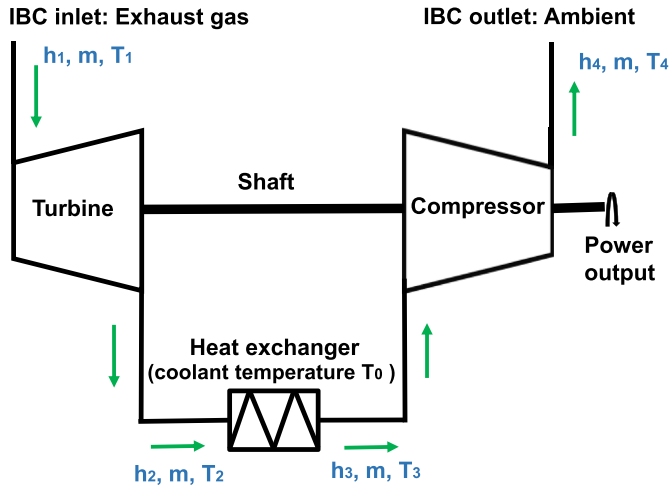

Fig. 3. A schematic diagram of a single-stage IBC system.

2.3. An asymmetric twin-scroll turbocharged diesel engine combining an IBC system

This work first presented a combined cycle of the asymmetric twin-scroll turbocharged diesel engine cycle and the inverse Brayton cycle. The schematic of a 6-cylinder asymmetric twin-scroll turbocharged diesel engine combining inverse Brayton cycle system is shown in Fig. 4. The combined cycle will further reduce NO_x emissions and increase both dynamic and fuel economy performances. The temperature-entropy diagram of the diesel engine with the combined cycle is shown in Fig. 5. The air first is boosted in the compressor (C_1) (1–2), and then cooled (2-2') in the intercooler. After entering the cylinders, it is pressured and burned to do work (3-4-5). When the exhaust gas is expanded in the ATST (5–6), it goes to the IBC system, and the exhaust energy can be

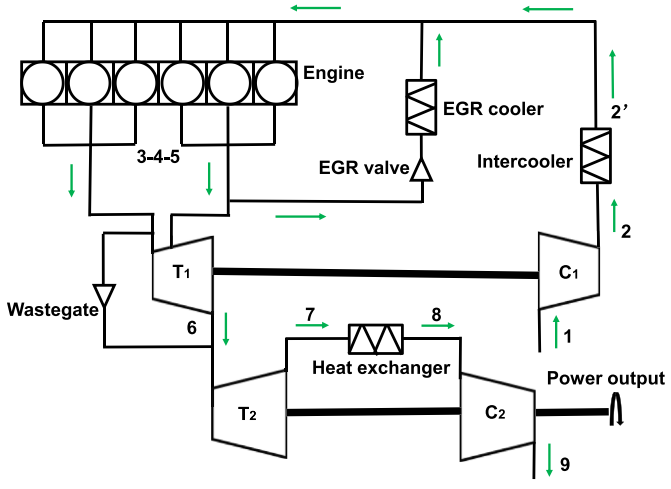

Fig. 4. A schematic diagram of a 6-cylinder asymmetric twin-scroll turbocharged diesel engine combining an IBC system.

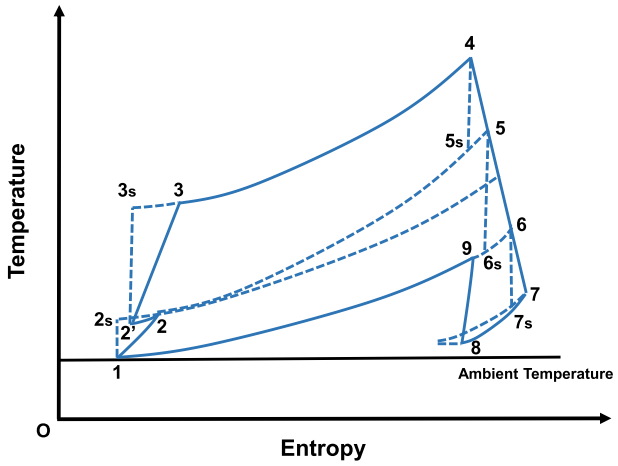

Fig. 5. Temperature-entropy diagram of the asymmetric twin-scroll turbocharged diesel engine combining an IBC system.

further recovered (6-7-8-9). Clearly, at the state 6, the exhaust gas expanded in the asymmetric twin-scroll turbine still carries a good deal of thermal energy, and it can be further recovered by the IBC system. Meanwhile, in the combined cycle, the EGR rate is also adjusted by the EGR valve.

3. Experimental and simulation methods

In this work, an experiment was conducted on a water-cooled, 12.55 L, 4-valve, 6-cylinder diesel engine equipped with an asymmetric twin-scroll turbocharging system (ASY = 53%) and an intercooled EGR system. The engine maximum torque and the rated power are 2380 Nm (1000–1400 rpm) and 351 kW (1900 rpm), respectively. The detailed test engine specifications are listed in Table 1. According to the schematic in Fig. 2, the whole experimental engine system was established on a dynamometer test bench. The primary testing tools are given in Table 2. The test engine operated at full load and at various speeds.

According to the experiment, Fig. 6 presents the engine simulation model that was developed and validated using the engine cycle simulation software (GT-SUITE v7.3.0). GT-SUITE, a registered trademark of Gamma Technologies, is commonly used for turbocharger matching and engine cycle simulation. GT-POWER is a significant part of GT-SUITE, and used to establish the engine numerical models. This software covers six aspects of the engine body, drive system, cooling system, fuel supply system, crankshaft mechanism, and valve mechanism. Meanwhile, it uses the finite volume method for fluid calculation, and has a powerful auxiliary modeling pre-processing tool, a wealth of combustion models and control functions, to effectively calculate engine torque, power, brake specific fuel consumption (BSFC) and other parameters.

In the model, the connecting pipes are simulated according to the experimental pipes. The length and shape are exactly the same, and the heat transfer and friction multipliers are set on the basis of the materials. For the EGR system, the model has one EGR circuit with the turbine small volute. The exhaust flow can be adjusted by the EGR valve, and meanwhile it must be cooled in the EGR cooler before back to the cylinders. In the asymmetric twin-scroll turbocharger model, an orifice joins the two entry pipes at the turbine inlet, and it can model backflow [46]. The compressor and turbine (ASY = 53%) maps are input, which are from turbocharger experiments shown in Fig. 7. For the engine system, it is a 6-cyclinder diesel engine with direct injection. The experimental engine operating conditions are presented in Table 3; these conditions were entirely adopted in the numerical models. The in-cylinder heat transfer is very significant, and the empirical WoschniGT (Eq. (8) and (9)) is applied. WoschniGT, a heat transfer model available in GT-POWER, has been used to model in-cylinder heat transfer. It indicates that the in-cylinder heat transfer will be calculated by a formula which closely emulates the classical Woschni correlation without swirl [47]. WoschniGT consists of two parts. First, the instantaneous average heat transfer coefficient for the working gas and chamber wall (α_g) can be calculated by Eq. (8). Then, the heat exchange for the gas and wall per unit engine crank angle ($\frac{dQw}{d\varphi}$) is naturally obtained using Eq. (9). The two formulas above will be used to calculate heat transfer from the engine cylinders and crankcase, which are very crucial for the engine output power and fuel consumption.

$$\alpha_g = 820 p^{0.8} T^{-0.53} D^{-0.2} \left[C_1 C_m + C_2 \frac{T_a V_s}{p_a V_a} (p - p_0) \right]^{0.8} \quad (8)$$

p, T – the working gas pressure and temperature

D – the cylinder diameter

C_m – the average piston speed

C_1 – the gas velocity coefficient

p_a, T_a, V_a – the working gas pressure, temperature and cylinder volume at the beginning of compression, respectively

p_0 – the cylinder pressure of the inverted engine

Table 1
Test engine specifications.

Items	Value and unit
Engine type	Inline 6-cylinder DI diesel
Number of valves per cylinder	4 (2 inlet/2 exhaust)
Bore	129 mm
Stroke	160 mm
Displacement	12.55 L
Compression ratio	18.2:1
Cooling system	Water cooled
Rated power	351 kW @1900 rpm
Maximum torque	2380 Nm @1000–1400 rpm
Air intake system	Intercooled asymmetric twin-scroll turbocharger (ASY = 53%)
EGR system	Intercooled EGR

Table 2
Test instrument specifications.

Instruments	Types (range and accuracy)
Eddy current dynamometer	C 500 (0–4000 Nm and 0–720 kW; ±10 rpm and ±1.25 Nm)
Fuel consumption measuring instrument	AVL735S (0.1–110 kg/h, 0.12%)
Data acquisition system	PUMA OPEN 1.2
Intake system	Sensyflow P/4000 (±5 mg)
Coolant constant temperature control device	AVL553 (70–120 °C)
Gas emission analyzer	MEXA-7100DEGR
Fuel constant temperature control device	AVL753 (15–80 °C)
Environment simulation system	ACS2400 (298 ± 1 K and 100 ± 1 kPa)

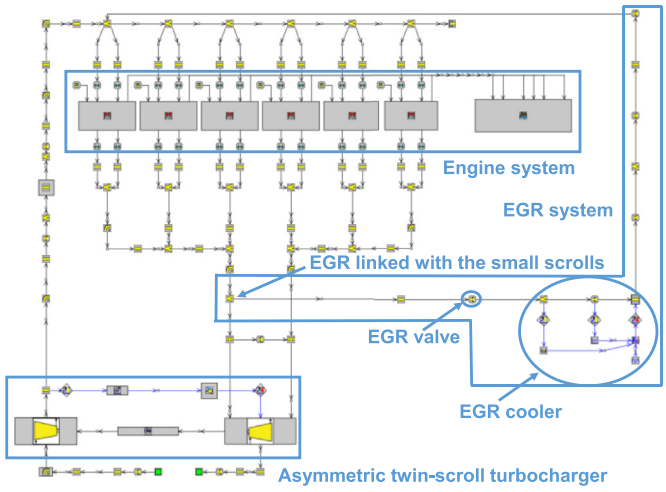

Fig. 6. Simulation model of the asymmetric twin-scroll turbocharged diesel engine.

$$\frac{dQw}{d\varphi}=\sum_{1}^{3}\frac{dQwi}{d\varphi}=\frac{1}{\theta}\sum_{1}^{3}\alpha g\cdot Ai(T-Twi)$$

θ – the angular velocity

A – the heat transfer area

Tw – the average wall temperature and = 1, 2 and 3 respectively represent the cylinder head, piston and cylinder liner. (9)

The most essential difference lies in the treatment of the heat transfer coefficients during the period when the valves are open; in this period, the heat transfer is increased by inflow velocities through the intake valves and by backflow through the exhaust valves. The heat transfer coefficient calculated using this model will decrease to zero as the engine speed decreases to zero. For all multi-zone combustion models, the convection temperature evaluation is calculated according to Eq. (10).

$$Tg=Tb\left(\frac{m_b}{m_t}\right)^n+Tu\left(1-\left(\frac{m_b}{m_t}\right)^n\right)$$

Tg – the effective gas temperature

Tb – the burned zone temperature (10)

Tu – the unburned zone temperature

m_b – the burned mass

m_t – the total mass

In which n is the weighting exponent that is calculated from linear to quadratic and the weighting exponent as follows:

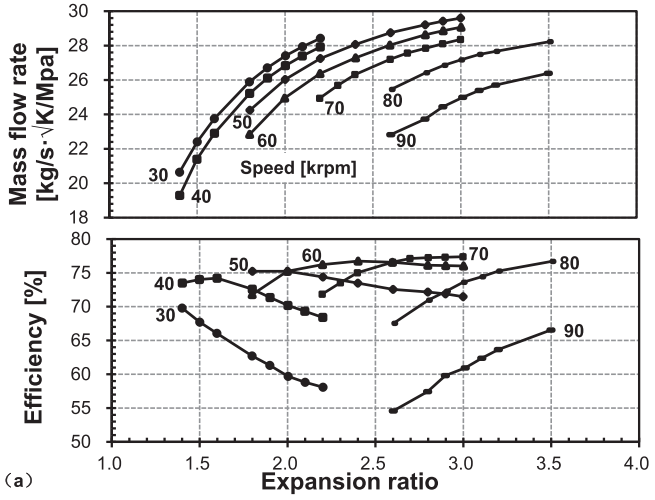

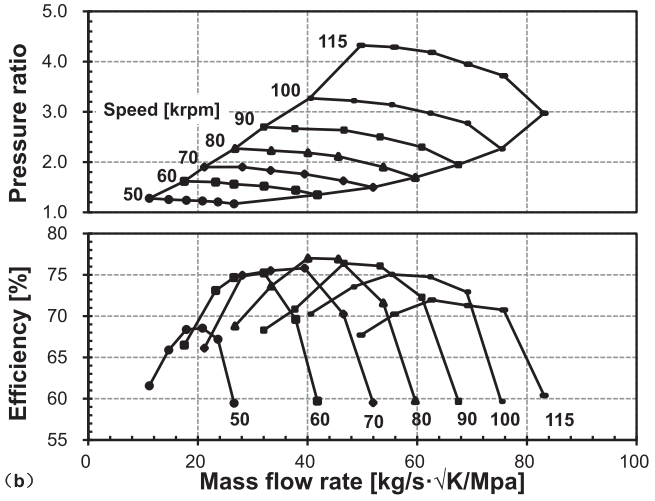

Fig. 7. The test asymmetric twin-scroll turbocharger maps: (a) turbine and (b) compressor.

$$n=1+\left(\frac{m_b}{m_t}\right)^2 \quad (11)$$

In Fig. 8, the validation of the engine performances are presented, including the turbine large scroll pressure, the small scroll pressure, the engine power, the EGR rate and the BSFC. The abscissa is the relative engine speed (RES), which is dimensionless to the maximum engine speed at the full load (1900 rpm). The ordinate is the engine relative performance, which is nondimensional to the

Table 3
Experimental engine operating conditions.

Speed (rpm)	Power (kW)	Atmospheric pressure (kPa)	Atmospheric temperature (K)	Atmospheric humidity (%)	Fuel mass (kg/h)
800	152	99.34	298.4	39.9	30.92
1000	250	99.31	298.6	40.7	48.72
1100	275	99.33	298.5	40.9	52.76
1200	300	99.33	298.1	40.8	57.68
1300	325	99.33	298.5	40.8	63.00
1400	350	99.30	298.6	40.8	68.85
1600	351	99.34	298.7	39.9	71.07
1900	350	99.37	298.8	38.4	75.52

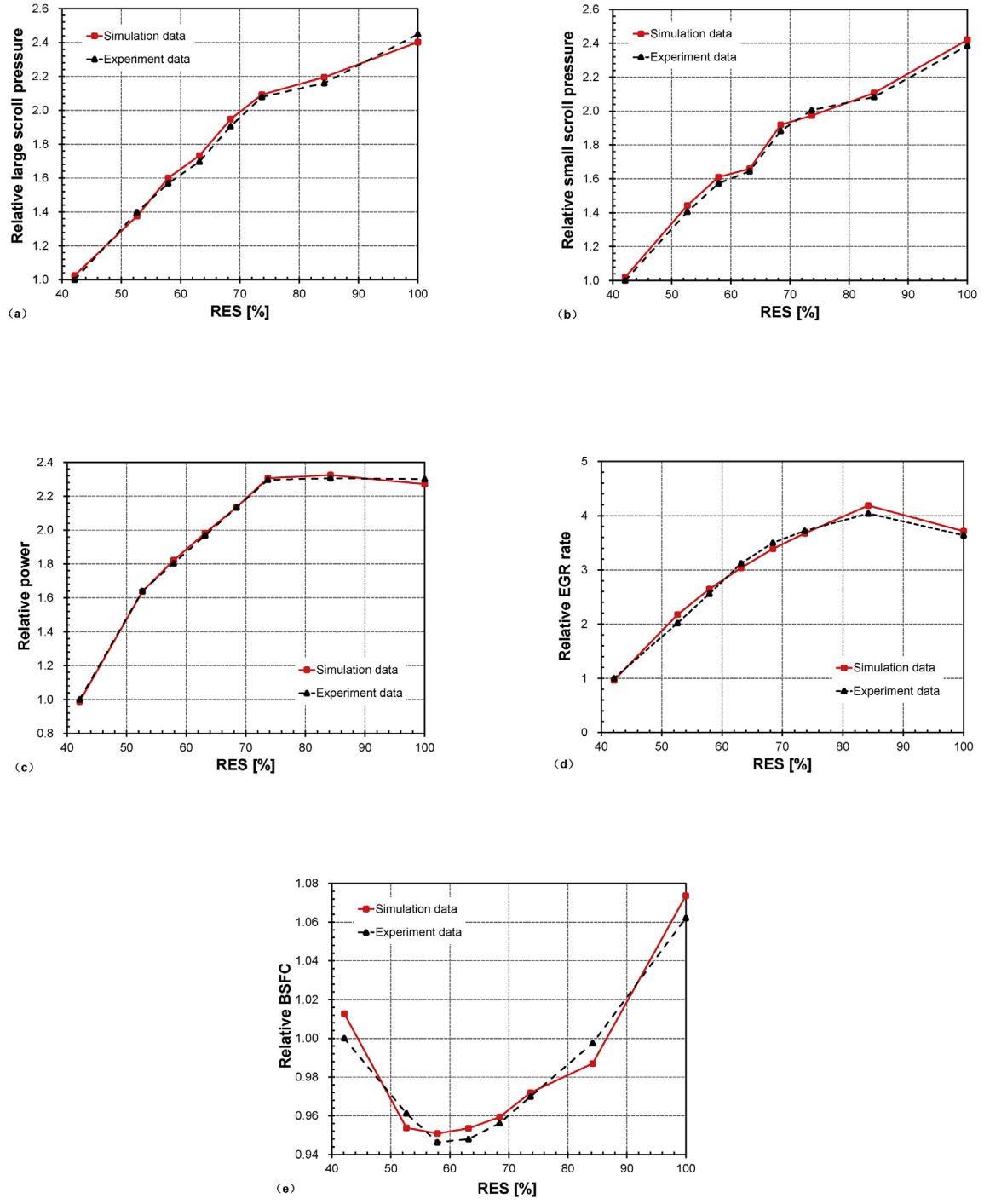

Fig. 8. Comparison of the simulation and experimental data: (a) large scroll pressure; (b) small scroll pressure; (c) engine power; (d) EGR rate and (e) BSFC.

experimental value at 800 rpm. The simulation results were found to agree well with the experimental data. For this study, the differences are considered to be acceptable.

This paper presents a proposed asymmetric twin-scroll turbocharged diesel engine combining an IBC system. The asymmetric twin-scroll turbocharging system is adopted to boost the intake gas and drive the EGR while achieving a lower fuel consumption, and the IBC system can further increase the utilization rate of the waste energy. Based on the model of Fig. 6, the numerical model of the engine system equipped with the combined cycle is established, as shown in Fig. 9. In particular, the diesel engine system and the asymmetric twin-scroll turbocharging system remain unchanged. In the IBC system, the compressor and the turbine maps are entered into the model by multiplying the turbocharger maps in Fig. 7. The heat exchanger can accurately control the outlet temperature by a PID device, and the effectiveness is 0.85.

4. Comparison of the combined cycle with the single cycle

In the combined cycle, the ASY of the asymmetric twin-scroll turbine and the throat area of the IBC turbine are two significant parameters used in the whole system matching process. In this section, the engine cycle simulation results of the combined cycle and single cycle are compared. To fully exploit the potential of the combined cycle, the effects of the two aforementioned critical parameters on the engine performances will be explored, and a comparison between the IBC and the power turbine will be discussed.

4.1. Influences of the key parameters on the engine performance

4.1.1. ASY of the asymmetric twin-scroll turbine

As mentioned earlier, ASY is a crucial parameter that characterizes the interrelationship of the two scrolls. In the combined cycle, the ASY determines the distribution of the exhaust flow for the two turbine volutes. In the asymmetric twin-scroll turbine model, the parameter “Map Fraction for Entry 1” (MF), which is set according to the turbine ASY (Eq. (12)), shows the difference between the throat areas of the two volutes. In the IBC turbine model, the turbine “Mass Multiplier” (TMP) represents the size of the throat area relative to the input map.

$$MF = \frac{ASY}{1 + ASY} \tag{12}$$

First, based on the models of the single cycle (Fig. 6) and the combined cycle (Fig. 9), engine cycle simulations were conducted. While ensuring that the two EGR valves remain fully open and the boost-pressure remains the same, both models were operated at full engine load while the ASY was changed from 40% to 70%. Moreover, the parameter TMP remained unchanged, and the value was set to 1.5. The output power of the engine is almost unchanged because of the same boost-pressure. The EGR rate differences between the combined cycle and the single cycle at different ASY from 40 to 100% RES are presented in Fig. 10. The results show that the engine speed and the ASY have great effects on the EGR rate. With the engine speed rising, the combined cycle has a higher EGR rate compared with that of the single cycle. At the low-range of the engine speed, the WG of the asymmetric twin-scroll turbine is completely closed as a means to boost the intake gas; therefore, in the combined cycle, the exhaust gas energy is rarely assigned to the IBC turbine and has little impact on the EGR rate. Beyond the engine maximum torque point, more exhaust energy from the WG of the asymmetric twin-scroll turbine is gradually produced, and the IBC turbine converts more exhaust heat into mechanical energy. Hence, the IBC turbine operates to influence both the outlet pressure of the asymmetric twin-scroll turbine and the EGR rate. Moreover, a smaller ASY creates further EGR rate improvements because the driving EGR pressure increases as ASY decreases. Taking two engine speeds as an example, the pressure differences between the intake and the small scroll in the combined cycle and single cycle versus the ASY range of 40–70% are shown in Fig. 11(a) (100% RES: the rated power point) and Fig. 11 (b) (58% RES: the maximum torque point). A large ASY corresponds to a larger throat area of the turbine small scroll; therefore, the small scroll pressure decreases with increasing ASY. The greater intake and the small scroll pressure difference in the combined cycle achieves maximum values of 1.63% (at 100% RES) and 0.72% (at 58% RES); thus, the maximum EGR difference is 2.96% at 100% RES (Fig. 10).

To exploit the potential of the combined cycle, it is necessary to achieve the same EGR rates at different engine speeds for the two types of cycles. First, the ASY of the single cycle is changed and the EGR rate is made the same as the combined cycle at the maximum torque point, because the it is the most demanding [35]. Generally,

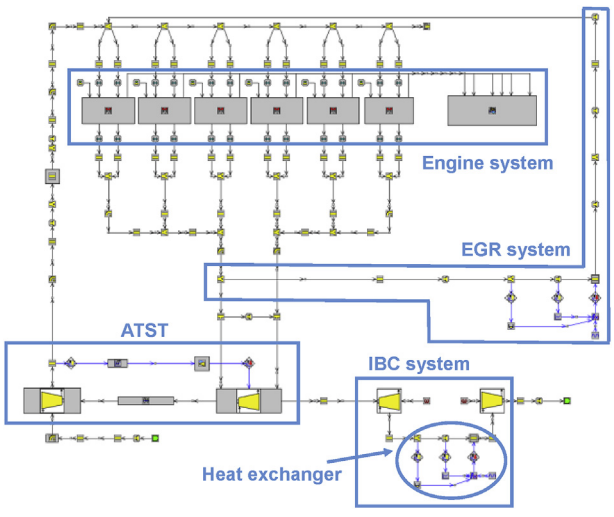

Fig. 9. Model of the asymmetric twin-scroll turbocharged diesel engine combining an IBC system.

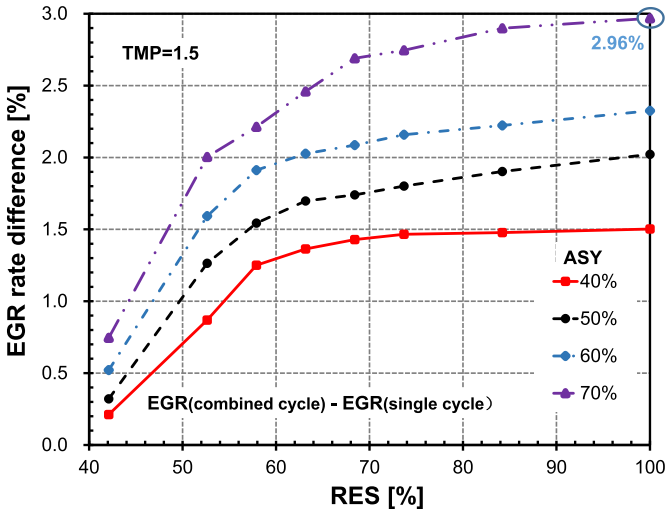

Fig. 10. The EGR rate differences between the combined cycle and the single cycle at 40–70% ASY and 40–100% RES.

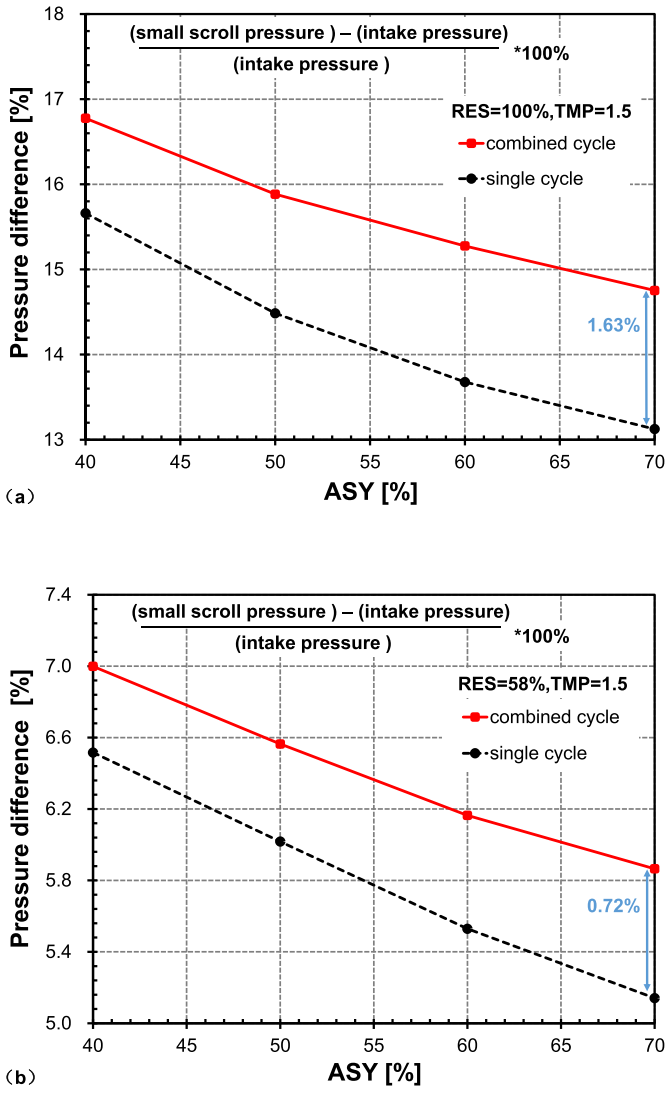

Fig. 11. The pressure differences between the intake and the small scroll in the combined cycle and single cycle versus the ASY range of 40–70%: (a) RES = 100%; (b) RES = 58%.

the ASY of the single cycle must be decreased to increase the EGR rate. At ASY = 50% and TMP = 1.5 of the combined cycle, the EGR rates with engine speeds when the EGR rate at the maximum torque point is adjusted to be the same are shown in Fig. 12. The two types of cycles are found to have different rising rules. The single cycle has smaller ASY and therefore has a higher EGR rate under the maximum torque point. Conversely, at the mid-range and high-range speeds, the single cycle presents the characteristic that the EGR rates of the combined cycle exceed those of the single cycle. To ensure the same EGR rate at different engine speeds, the EGR valve opening degree (OPD) must be properly set. In Fig. 13, at low speeds, the EGR valve of the combined cycle and the single cycle is fully open and partially open, respectively. The regulation law is the opposite beyond 58% RES.

For 40–70% ASY in the combined cycle, the ASY correspondence in the single cycle is presented in Fig. 14. Each point on the line indicates the two types of cycles have the same EGR rate at the maximum torque point. Given the same EGR rates by changing OPD, Fig. 15 suggests that power improvement PI of the combined cycle is achieved at 40–70% ASY and 40–100% RES compared with the single cycle. According to Eq. (7), the power improvement is defined as follows:

$$\mathrm{PI} = \frac{P_{cc} + P_{IBC} - P_{sc}}{P_{sc}} \times 100\% \tag{13}$$

where P_{cc} is the power of the engine with the combined cycle, and P_{sc} is the power of the engine with the single cycle. The result shows that the combined cycle has a better dynamic property compared with the single cycle. A smaller ASY will improve the PI. For the single cycle, the gas exchange condition will deteriorate when the ASY decreases while the redundant exhaust gas energy will be recovered in the IBC system. Meanwhile, at low speeds, most of the exhaust energy needs to pressure the intake gas. With increasing engine speeds, the exhaust gas temperature will rise, and more exhaust energy will boost the IBC system, and therefore PI will increase. The PI value is in the range of about 1.00% and 5.00%, and reaches a maximum value at 40% ASY and 100% RES.

4.1.2. IBC turbine's throat area

For the performance of the engine with the combined cycle, the IBC turbine's throat area determines the back-pressure of the ATST and the power improvement of the IBC system. Thus, it is very

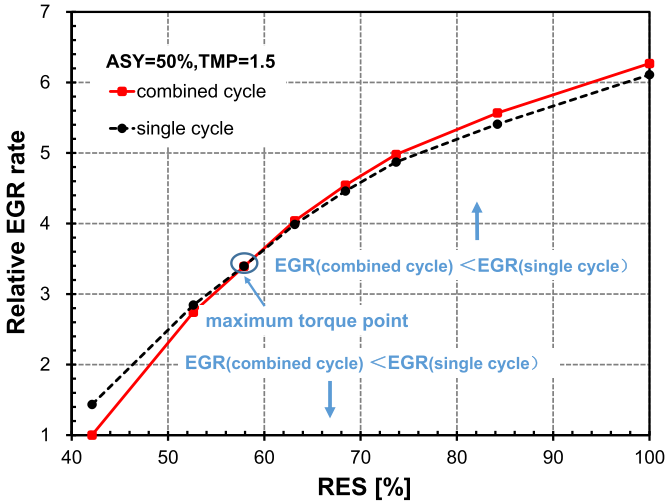

Fig. 12. EGR rates with engine speeds at ASY = 50% and TMP = 1.5 of the combined cycle when the EGR rate at the maximum torque point is the same.

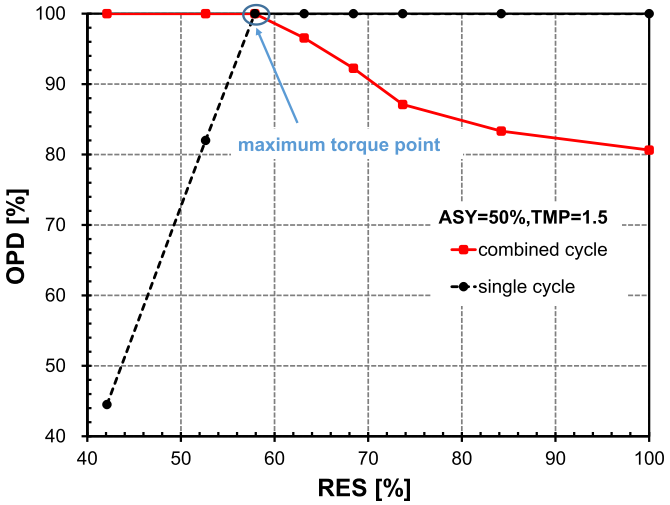

Fig. 13. OPD relationship at ASY = 50% and TMP = 1.5 of the combined cycle when the EGR rates are the same at different engine speeds.

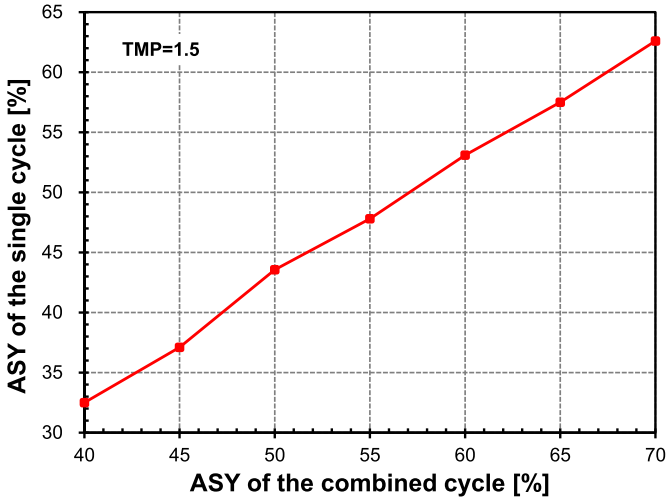

Fig. 14. ASY correspondence of the combined cycle and the single cycle at the same EGR rates.

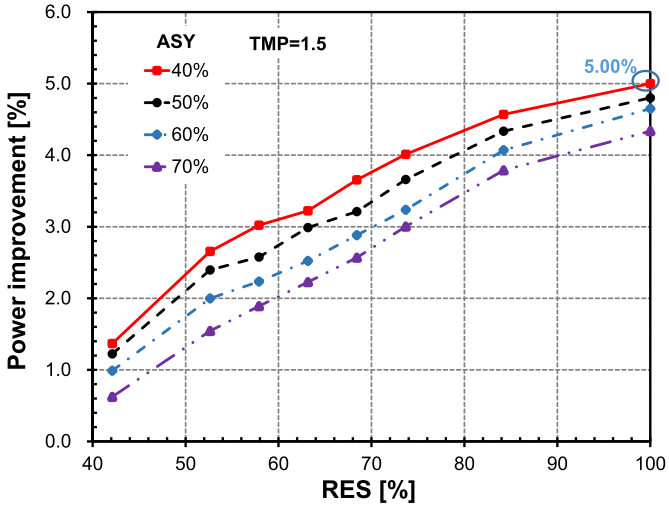

Fig. 15. Power improvements of the combined cycle at 40–70% ASY and 40–100% RES compared with the single cycle.

significant to study the effect of the IBC turbine's throat area on the engine performance. The value of TMP reflects the turbine size.

In the models of the combined cycle, only the TMP is changed; the turbine expansion ratio and efficiency remain unchanged. In Fig. 16, the EGR rate differences between the combined cycle and the single cycle at 1.2–1.8 TMP and 40–100% RES when the ASY is fixed to 50% are illustrated. The results suggest that a smaller TMP will bring improvements to EGR rates, and the maximum EGR rate difference reaches 3.66%. A smaller TMP indicates that the whole exhaust passage throat area decreases to increase the exhaust back-pressure. The pressure difference of the small scroll and the intake reduces with the increasing of TMP in the two types of cycles are shown in Fig. 17. The condition of 100% and 58% RES maximizes the values of 3.07% and 1.24%, respectively. In the simulation models, the engine intake gas pressure is controlled by a PID device. If the boost-pressure exceeds the set point, then the PID device will command the turbine WG to open. In other words, the IBC turbine's throat area has great influence on the engine exhaust back-pressure.

To ensure the same EGR rate at the maximum torque point, the

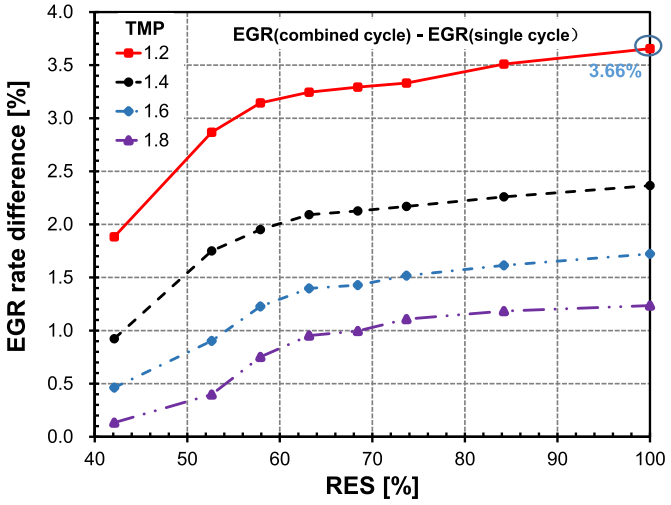

Fig. 16. The EGR rate differences between the combined cycle and the single cycle at 1.2–1.8 TMP and 40–100% RES.

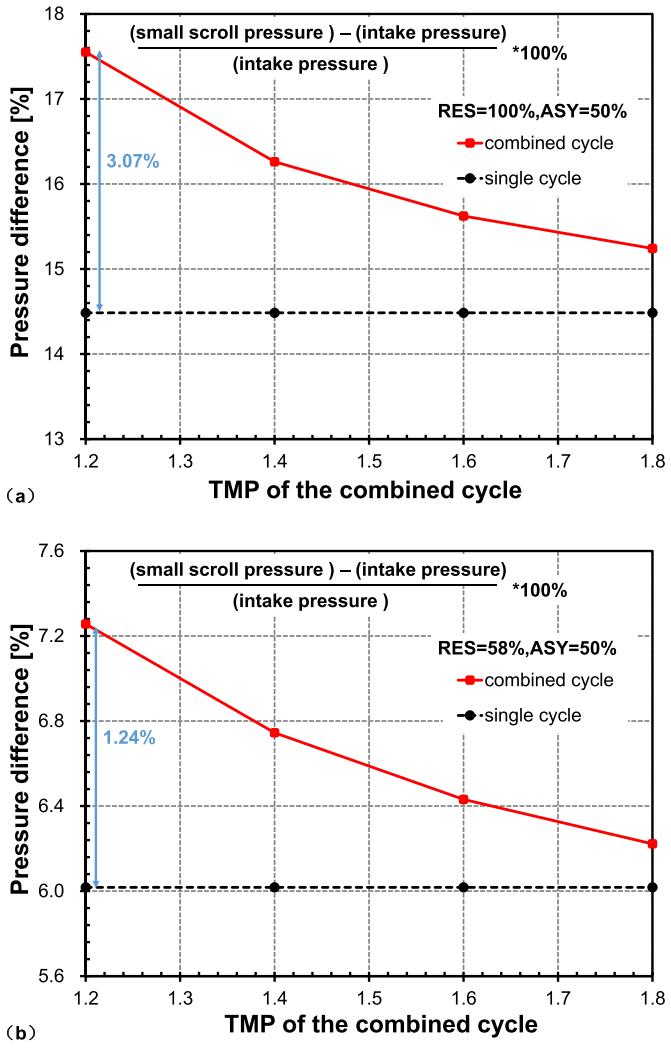

Fig. 17. The pressure differences between the intake and the small scroll in the combined cycle and single cycle versus the TMP range of 1.2–1.8: (a) RES = 100%; (b) RES = 58%.

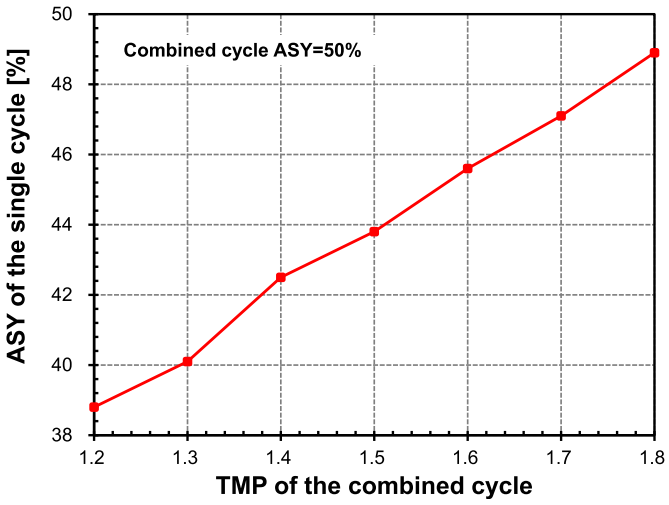

Fig. 18. ASY of the single cycle versus 1.2–1.8 TMP at the same EGR rates.

single cycle must decrease ASY for a higher EGR rate. When the ASY is 50% in the combined cycle, the ASY of the single cycle versus the TMP is given as shown in Fig. 18. It is clearly demonstrated that the ASY of the single cycle grows almost linearly with the TMP of the combined cycle, and a TMP growth of 0.1 will require the single cycle ASY to increase by approximately 1.7%. Similarly, when the EGR rate is at the maximum torque point in the two types of cycles, the OPD is adjusted to achieve the appropriate EGR rates over the entire range of operating conditions. The PI between the two cycles at different TMP settings is shown in Fig. 19. As already mentioned, the PI will go up with increasing engine speeds. Meanwhile, a smaller TMP makes the gas exchange condition worse, thereby reducing engine performance. The PI value is in the range of about 0 and 5.78%, and reaches a maximum value at 1.8 TMP and 100% RES. However, for the combined cycle, the TMP should be chosen properly to achieve the balance between the EGR rate and the system power.

4.2. Discussion of the combined cycle and the power turbine

At present, a turbo-compounding system is a promising technology for use in the exhaust energy recovery and enhancing fuel economy. Turbocharging comes in many forms; one form, named the power turbine, can be placed with the turbocharger turbine in series or in parallel, or even integrated with the turbocharger [48,49]. In Fig. 20 (a), a 6-cylinder asymmetric twin-scroll turbocharged diesel engine combining a power turbine system in series is presented. Hountalas et al. [50] performed a thorough investigation using modeling to estimate the potential of energy recovery from the exhaust of a heavy-duty diesel engine using turbo-compounding. Mamat et al. [51] found the low pressure available to the exhaust gases expanded in the main turbocharger and that a constant rotational speed is required by the electric motor; their findings motivated the design of a new turbine that provided a high performance at lower pressures.

Based on Fig. 6, the GT-POWER model of the engine with the power turbine is developed in Fig. 20 (b). Under the same EGR rate and 50% ASY, the power improvements of the power turbine and the combined cycle are shown in Fig. 21. It can be known the combined cycle have power advantages versus the power turbine. At low speeds, the power turbine has almost no power revenue, and meanwhile it has the maximum power improvement of 3.95% which is also lower than the combined cycle. In the power turbine system, the power turbine operation requires that the inlet

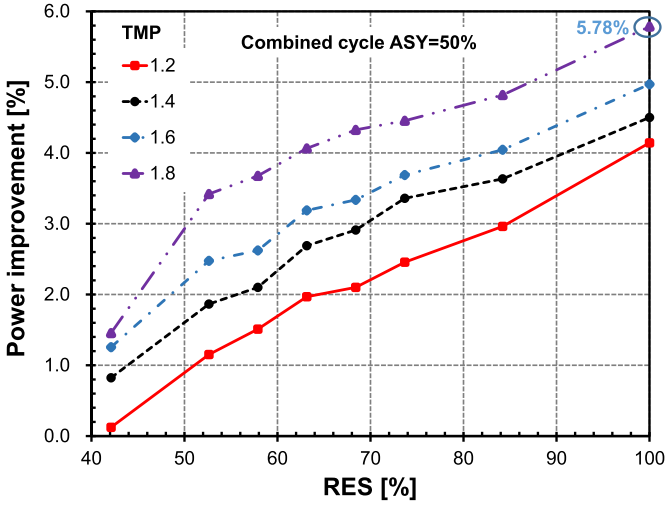

Fig. 19. Power improvements of the combined cycle at 1.2–1.8 TMP and 40–100% RES compared with the single cycle.

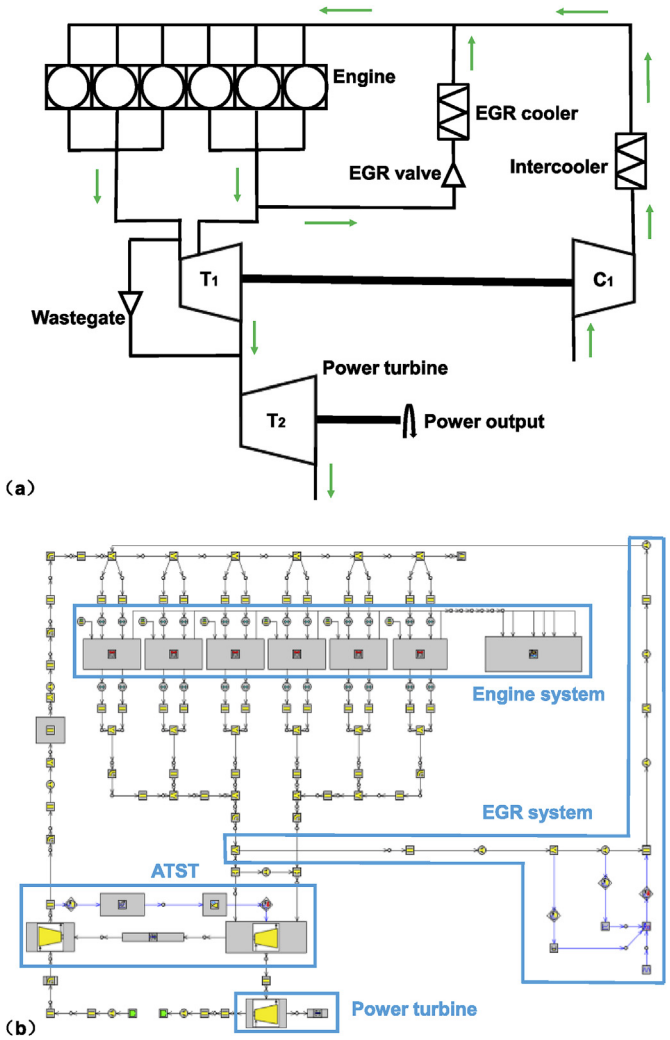

Fig. 20. A 6-cylinder asymmetric twin-scroll turbocharged diesel engine combining a power turbine system: (a) the schematic diagram, and (b) the GT-POWER model.

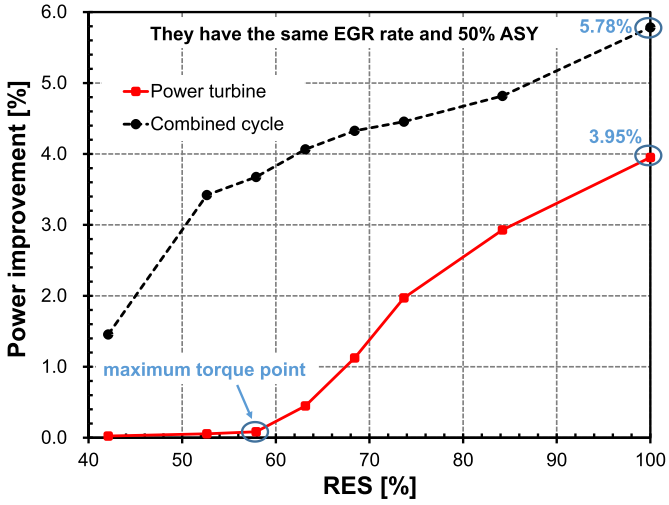

Fig. 21. Power improvements of the power turbine and the combined cycle under the same EGR rate and 50% ASY.

pressure (p_3) be higher than atmospheric pressure (p_0). Generally, the power turbine plays a significant role at the high-range of the engine speed, because at low and medium speeds, most of the exhaust energy is used to boost the intake gas. However, in the IBC system (Fig. 4), p_3 could be smaller than p_0 because the system produces an under atmospheric pressure condition.

(1) When $p_3 \leq p_0$, the power turbine cannot operate and the IBC turbine can achieve further absorption of both waste heat pressure energy.
(2) When $p_3 > p_0$, the expansion ratio of the power turbine ($\frac{p_3}{p_0}$) and the expansion ratio of the IBC turbine ($\frac{p_3}{p_4}$) have the following relationship:

$$\frac{p_3}{p_0} \leq \frac{p_3}{p_4} \tag{14}$$

Therefore, the IBC system has better performance, especially at the low-speed of an engine; this characteristic is very important for heavy-duty diesel engines, which have high requirements for the low-speed torque.

5. Conclusions and remarks

A new combined cycle involving the asymmetric twin-scroll turbocharged diesel engine cycle and the inverse Brayton cycle was first proposed to achieve engine performance improvements. To adequately excavate its potential on energy and emissions, this study established and validated the two numerical models of the combined cycle and the single cycle according to experimental results. The engine performances were compared under the changes of the two important parameters of the degree of asymmetric turbine asymmetry and the IBC turbine's throat area, and the advantage of the combined cycle compared with the power turbine was also discussed. The most significant results are the following:

(1) The turbine ASY has a great effect on the engine performances of the combined cycle and the single cycle. The former engine was found to have an improvement EGR rate compared to the latter engine at different values of ASY. Given the same EGR rates at different engine speeds, the power improvement of the combined cycle increases with increasing engine speed and decreasing ASY, reaching a maximum of 5.00% at 40% ASY and 100% RES.
(2) The IBC turbine throat area influences the power distribution in the combined cycle. A smaller throat area produces a higher pressure difference between the small scroll and the intake, resulting in higher EGR rates. Further power improvements are achieved with increasing throat area when the EGR rates of the combined cycle and the single cycle are adjusted to be the same, reaching the maximum value of 5.78% at 1.8 TMP and 100% RES.
(3) Compared with the single cycle and the power turbine, the combined cycle has certain advantages. Improvements in the EGR rate and power are achieved between the combined and single cycles. Additionally, the IBC system can utilize more waste heat at low and medium engine speeds than the power turbine, making it well-suited for use in heavy-duty diesel engines.

The results of this study showed that the combined cycle had more improvements on engine EGR rate and output power. Different operations of the engine will be planned for further study and test to reduce engine emissions and increase energy efficiency. More research will be needed if engineering applications are to be implemented.

Acknowledgments

This research was supported by the National Natural Science Foundation of China (Grant No. 51876097).

References

[1] Rabih O, Rafic Y, Jean-Claude C, Rachid O. New indicated mean effective pressure (IMEP) model for predicting crankshaft movement. Energy Convers Manag 2013;52:3376–82.
[2] Kai M, Al-Abdullah M, Alzubail A, Kalghatgi G, Viollet Y, Head R, Khan A, Abdul-Manan M. Synergistic engine-fuel technologies for light-duty vehicles: fuel economy and Greenhouse Gas emissions. Appl Energy 2017;208:1538–61.
[3] Hogg R. Life beyond euro VI. 2014. Last accessed 13.07.15, http://www.automotiveworld.com/megatrends-articles/life-beyond-euro-vi/.
[4] Padzillah MH, Rajoo S, Martinez-Botas RF. Influence of speed and frequency towards the automotive turbocharger turbine performance under pulsating flow conditions. Energy Convers Manag 2014;80:416–28.
[5] Galindo J, Tiseira A, Fajardo P, García-Cuevas LM. Development and validation of a radial variable geometry turbine model for transient pulsating flow applications. Energy Convers Manag 2014;85:190–203.
[6] Raptotasios SI, Sakellaridis NF, Papagiannakis RG, Hountalas DT. Application of a multi-zone combustion model to investigate the NO_x reduction potential of two-stroke marine diesel engines using EGR. Appl Energy 2015;157:814–23.
[7] Li W, Liu Z, Wang Z, Dou H. Experimental and theoretical analysis of effects of atomic, diatomic and polyatomic inert gases in air and EGR on mixture properties, combustion, thermal efficiency and NO_x emissions of a pilot-ignited NG engine. Energy Convers Manag 2015;105:1082–95.
[8] Zhong L, Musial M, Reese R, Black G. EGR systems evaluation in turbocharged engines. SAE technical paper 2013-01-0936.
[9] Taghavifar H, Taghavifar H, Mardani A, Mohebbi A. Modeling the impact of in-cylinder combustion parameters of DI engines on soot and NO_x emissions at rated EGR levels using ANN approach. Energy Convers Manag 2014;87:1–9.
[10] Huang H, Liu Q, Wang Q, Zhou C, Mo C, Wang X. Experimental investigation of particle emissions under different EGR ratios on a diesel engine fueled by blends of diesel/gasoline/n -butanol. Energy Convers Manag 2016;121:212–23.
[11] Divekar PS, Chen X, Tjong J, Zheng M. Energy efficiency impact of EGR on organizing clean combustion in diesel engines. Energy Convers Manag 2016;112:369–81.
[12] Roy S, Ghosh A, Das AK, Banerjee R. Development and validation of a GEP model to predict the performance and exhaust emission parameters of a CRDI assisted single cylinder diesel engine coupled with EGR. Appl Energy 2015;140:52–64.
[13] Zamboni G, Capobianco M. Influence of high and low pressure EGR and VGT control on in-cylinder pressure diagrams and rate of heat release in an automotive turbocharged diesel engine. Appl Therm Eng 2013;51(1–2):586–96.
[14] Aghaali H, Ångström HE. A review of turbocompounding as a waste heat

recoverysystem for internal combustion engines. Renew Sustain Energy Rev 2015;49:813–24.
[15] Taghavifar H, Khalilarya S, Jafarmadar S. Exergy analysis of combustion in VGT-modified diesel engine with detailed chemical kinetics mechanism. Energy 2015;93:740–8.
[16] Saidur R, Rezaei M, Muzammil WK, Hassan MH, Paria S, Hasanuzzaman M. Technologies to recover exhaust heat from internal combustion engines. Renew Sustain Energy Rev 2012;16:5649–59.
[17] Hatami M, Cuijpers MCM, Boot MD. Experimental optimization of the vanes geometry for a variable geometry turbocharger (VGT) using a Design of Experiment (DoE) approach. Energy Convers Manag 2015;106:1057–70.
[18] Mao B, Yao M, Zheng Z, Liu H. Effects of dual loop EGR and variable geometry turbocharger on performance and emissions of a diesel engine. SAE technical paper 2016-01-2340.
[19] Aghav Y, Kumar MN, Latey AA, Gandhi N, Gokhale N. Development of two stage turbo-charging for medium duty diesel engine of power generation application. SAE technical paper 2012-28-0007.
[20] Cui Y, Hu Z, Deng K, Wang Q. Miller-cycle regulatable, two-stage turbocharging system design for marine diesel engines. J Eng Gas Turbines Power 2014;136:505–13.
[21] Galindo J, Serrano JR, Climent H, Varnier O. Impact of two-stage turbocharging architectures on pumping losses of automotive engines based on an analytical model. Energy Convers Manag 2010;51(10):1958–69.
[22] Zheng Z, Feng H, Mao B, Liu H, Yao M. A theoretical and experimental study on the effects of parameters of two-stage turbocharging system on performance of a heavy-duty diesel engine. Appl Therm Eng 2018;129:822–32.
[23] Martinez-Botas RF, Pesiridis A, Yang MY. Overview of boosting options for future downsized engines. Sci China Technol Sci 2011;54:318–31.
[24] Furukawa H, Yamaguchi H, Takagi K, Okita A. Reliability on variable geometry turbine turbocharger. 1993. SAE technical paper 930194.
[25] Westin F, Burenius R. Measurement of interstage losses of a twostage turbocharger system in a turbocharger test rig. SAE technical paper 2010-01-1221.
[26] Schorn NA. The radial turbine for small turbocharger applications: evolution and analytical methods for twin-entry turbine turbochargers. SAE Int J Engines 2014;27(3):1422–42.
[27] Chiong MS, Rajoo S, Romagnoli A, Costall AW, Martinez-Botas RF. Non-adiabatic pressure loss boundary condition for modelling turbocharger turbine pulsating flow. Energy Convers Manag 2015;93:267–81.
[28] Chiong MS, Rajoo S, Romagnoli A, Costall AW, Martinez-Botas RF. One-dimensional pulse-flow modeling of a twin-scroll turbine. Energy 2016;115:1291–304.
[29] Copeland CD, Newton PJ, Martinez-Botas R, Seiler M. The effect of unequal admission on the performance and loss generation in a double-entry turbocharger turbine. Proceedings of the ASME turbo expo 2010: power for land, sea and air. 2010. Paper GT2010-22212.
[30] Müller M, Streule T, Sumser S, Hertweck G, Nolte A, Schmid W. The asymmetric twin scroll turbine for exhaust gas turbochargers. In: Proceedings of the ASME turbo expo 2008: power for land, sea and air; 2008. Paper GT2008-50614.
[31] Hoffmann K, Benz M, Weirich M, Herrmann HO. The new Mercedes-Benz medium duty commercial natural gas engine. Mtz Worldwide 2014;75(11):4–11.
[32] Nielsen B, Sladek W, Müller M, Eberle F. The latest heavy-duty engine generation from Mercedes-Benz — part 1: aims and design. Mtz Worldwide 2016;77(6):48–53.
[33] Schmidt S, Rose MG, Müller M, Sumser S, Chebli E, Streule T, Stiller M, Leweux J. Variable asymmetric turbine for heavy duty truck engines. In: Proceedings of the ASME turbo expo 2013: turbine technical conference and exposition; 2013. Paper GT2013-94590.
[34] Ernst M, Kleffel J, Koch D. The latest generation of Daimler's 10.7 l heavy-duty engine. Internationaler Motorenkongress 2017.
[35] Zhu D, Zheng X. Asymmetric twin-scroll turbocharging in diesel engines for energy and emission improvement. Energy 2017;141:702–14.
[36] Zhu D, Zheng X. A new asymmetric twin-scroll turbine with two wastegates for energy improvements in diesel engines. Appl Energy 2018;233:263–72.
[37] Kennedy I, Chen Z, Ceen B, Jones S, Copeland CD. Experimental investigation of an inverted brayton cycle for exhaust gas energy recovery. In: Proceedings of the ASME turbo expo 2013: turbine technical conference and exposition; 2018. Paper GT2018-75386.
[38] Wilson GD. The design of high-efficiency turbomachinery and gas turbines. MIT press; 1984.
[39] Agnew B, Anderson A, Potts I, Frost TH, Alabdoadaim MA. Simulation of combined Brayton and inverse Brayton cycles. Appl Therm Eng 2003;23(8):953–63.
[40] Bianchi M, Montenegro GND, Peretto A, Spina PR. A feasibility study of inverted Brayton cycle for gas turbine repowering. J Eng Gas Turbines Power 2005;127(3):599–605.
[41] Zhang W, Chen L, Sun F. Power and efficiency optimization for combined Brayton and inverse Brayton cycles. Appl Therm Eng 2009;29:2885–94.
[42] Goodarzi M, Kiasat M, Khalilidehkordi E. Performance analysis of a modified regenerative Brayton and inverse Brayton cycle. Energy 2014;72(7):35–43.
[43] Copeland CD, Chen Z. The benefits of an inverted Brayton bottoming cycle as an alternative to turbo-compounding. In: Proceedings of the ASME turbo expo 2015: turbomachinery technical conference and exposition; 2015. Paper GT2015-42623.
[44] Chen Z, Copeland CD. Inverted Brayton cycle employment for a highly downsized turbocharged gasoline engine. In: SAE Int Powertrains Fuels Lubricants Meeting 2015-01-1973; 2015.
[45] Palenschat T, Mueller M, Rajoo S, Chiong MS, Newton P, Martinez-Botas R, Tan F. Steady-state experimental and meanline study of an asymmetric twin-scroll turbine at full and unequal and partial admission conditions. SAE technical paper 2018-01-0971.
[46] Uhlmann T, Lückmann D, Aymanns R, Scharf J, Höpke B, Scassa M, Rütten O, Schorn N, Kindl H. Development and matching of double entry turbines for the next generation of highly boosted gasoline engines. XXII Simpósio Internacional de Engenharia Automotiva; 2014. p. 777–814.
[47] Lahuerta J, Samuel S. Numerical simulation of warm-up characteristics and thermal management of a GDI engine. SAE technical paper; 2013-01-0870.
[48] Zhao R, Zhuge W, Zhang Y, Yin R, Chen Z, Li Z. Parametric study of power turbine for diesel engine waste heat recovery. Appl Therm Eng 2014;67(1–2):308–19.
[49] Davorin K. Turbo-hydraulic engine exhaust power recovery system, SAE technical paper, 2002-01-2731.
[50] Hountalas DT, Katsanos CO, Lamaris VT. Recovering energy from the diesel engine exhaust using mechanical and electrical turbocompounding. SAE technical paper, 2007-01-1563.
[51] Mamat AMI, Padzillah MH, Romagnoli A, Martinez-Botas RF. A high performance low pressure ratio turbine for engine electric turbocompounding. In: Proceedings of the ASME turbo expo 2011: power for land, sea and air; 2011. Paper GT2011-45541.

Nomenclature

h: enthalpy (kJ/kg)
m: mass flow rate (kg/s)
rpm: revolutions per minute
rps: revolutions per second
P: power (kW)
η: isentropic efficiency

Subscripts

c: compressor
i: engine intake
l: turbine large scroll
s: turbine small scroll
t: turbine

Abbreviations

ASY: turbine asymmetry
ATST: asymmetric twin-scroll turbine
BC: Brayton cycle
BSFC: brake specific fuel consumption
C: compressor
DI: direct injection
EGR: exhaust gas recirculation
IBC: inverse Brayton cycle
NO_x: nitrogen oxides
OPD: opening degree of the EGR valve
PI: power improvement
RES: relative engine speed
SI: spark ignition
T: turbine
TA: throat area
TMP: IBC turbine “Mass Multiplier”
VGT: variable geometry turbine
WG: wastegate